crystals

MDPI

Article

Two-Dimensional Hydrogen-Bonded Crystal Structure, Hirshfeld Surface Analysis and Morphology Prediction of a New Polymorph of 1H-Nicotineamidium Chloride Salt

Hela Ferjani [1], Hammouda Chebbi [2,*], Abderrahmen Guesmi [2], Obaid S. AlRuqi [3] and Sami A. Al-Hussain [1]

[1] Chemistry Department, College of Science, IMSIU (Imam Mohammad Ibn Saud Islamic University), Riyadh 11623, Saudi Arabia; hhferjani@imamu.edu.sa (H.F.); sahussain@imamu.edu.sa (S.A.A.-H.)

[2] Chemistry Department, Faculty of Sciences of Tunis, Laboratory of Materials, Crystal Chemistry and Applied Thermodynamics, Tunis El Manar University, El Manar II 2092, Tunisia; abderrahmen.guesmi@ipeim.rnu.tn

[3] Department of Pharmaceutical Chemistry, College of Pharmacy, King Saud University, P.O. Box 2457, Riyadh 11451, Saudi Arabia; oalroqi@ksu.edu.sa

* Correspondence: chebhamouda@yahoo.fr

Received: 14 September 2019; Accepted: 28 October 2019; Published: 31 October 2019

Abstract: A new polymorph of 1H-nicotineamidium chloride salt, $(C_6H_7N_2O)^+ \cdot Cl^-$, was grown by slow evaporation at room temperature. It crystallizes in the monoclinic space group $P2_1/m$. The crystal structure study shows that the organic cations $(C_6H_7N_2O)^+$ and chloride anions are organized into 2D-layers packed along the *b*-axis. The structural components interact by N–H···O, N–H···Cl and C–H···Cl hydrogen bonds building up a two-dimensional network. The protonated organic cations and the chloride anions show a π–Cl^- interaction enhancing stability to the crystal structure. A description of the hydrogen-bonding network and comparison with similar related compounds of nicotinamide and isonicotineamide are presented. The bulk morphology was also predicted and it was found that the simulated morphology predicted by Bravais–Friedel–Donnay–Harker (BFDH) model matches with the morphology of as grown single crystal. Moreover, to illustrate the intermolecular interactions in the new studied polymorph, we report also the analysis of the Hirshfeld surface and its fingerprint polts.

Keywords: crystal structure; new polymorph; 1H-Nicotineamide; hirshfeld surface analysis; BFDH morphology prediction

1. Introduction

Crystalline organic materials are being actively explored for potential application in optoelectronics and as piezoelectric and other type of functional materials [1,2]. To realize the potential of crystalline organic materials in materials science, it would be helpful to be able to correlate molecular structure, crystalline structure and macroscopic properties to "design" materials. Reasons behind a specific arrangement of molecules inside a crystal structure are usually concluded from the arrangement and nature of intermolecular interactions, and are sometimes sustained by theoretical calculations [3,4]. In many cases, these interactions take the form of 1D, 2D or 3D hydrogen bond networks joining charged or neutral molecules [5,6]. Stability, solubility and structure of a crystalline solid depend on the overall system of intermolecular/interionic interactions, among which multiple hydrogen bonds play a very important role.

Apart from those, the selection of nicotinamide as an excellent crystallizing compound is a key for the construction of unusual salts and cocrystals. It has two hydrogen bonding groups suitable for

the formation of an intermolecular skeleton. The amide group has two sites of hydrogen bonding interactions and two lone pairs on the carbonyl oxygen atom. A second hydrogen bond acceptor is the lone pair on the N atom of the pyridine ring. This makes the molecule very flexible for a variety of hydrogen bonded interactions, particularly in pharmaceutical co-crystals [7–11]. Our objective is to gain a better vision into the structural chemistry of a new polymorph of 1H-nicotineamidium chloride salt as well as its control on the overall structure. Therefore, we cultivate the morphology of 1H-nicotineamidium chloride by computer software. We found that the result was then compared on the basis of their most relevant characteristics. Moreover, the experimental and the predicted crystal morphologies calculation using Bravais–Friedel–Donnay–Harker (BFDH) model reveals similarities. The global intermolecular interactions involved in the structure were quantified and fully explained by Hirshfeld surface analysis.

2. Experimental

2.1. Synthesis

The 1H-Nicotineamidium chloride compound $(C_6H_7N_2O)^+ \cdot Cl^-$ was synthesized by slow evaporation of aqueous solution containing a 1:1 stoichiometric mixture of 1H-nicotineamide and concentrated HCl (37%). The resulting solution was stirred well then kept at room temperature. After a period of about three weeks, bulk colorless crystals were obtained. A single crystal suitable for X-ray diffraction analysis was selected and studied.

2.2. The SEM Technique

The scanning electron microscopy (SEM) technique (JEOL, JSM-6380-LA) was applied to observe the morphology of the crystallized salt. The working distance was 15 mm with an accelerating voltage of 10 kV.

2.3. X-ray Crystallography and Data Collection

A single colorless crystal of dimensions $0.32 \times 0.21 \times 0.12$ mm^3 of the title compound was selected and X-ray intensity data were collected at 298 K on a Bruker SMART APEXII D8 venture single crystal diffraction system equipped with a graphite monochromatic, using Mo-Kα radiation (λ = 0.71073 Å). The structure was solved and refined by full-matrix least squares based on F^2 using SHELXT [12] and SHELXL [13] respectively. All atoms were positioned from Fourier difference maps after looking to the bond length calculations. The atomic positions were refined with anisotropic displacement parameters. Hydrogen coordinates were idealized using appropriate HFIX instructions and included in subsequent least-squares refinement cycles in a riding motion approximation. Molecular graphics were prepared using Diamond 3 [14]. Crystal data and experimental parameters used for the intensity data collection are summarized in Table 1.

Table 1. Crystallographic parameters and data collection for $(C_6H_7N_2O)^+$ Cl.

Crystal Data	
Empirical Formula	$C_6H_7ClN_2O$
Formula Weight (g mol^{-1})	158.59
Crystal System, Space Group	Monoclinic, $P2_1/m$
a (Å)	7.1671(4)
b (Å)	6.6664(3)
c (Å)	7.4883(4)
V (Å^3)	352.84(3)
β	99.531(2)
Z	2

Table 1. *Cont.*

Crystal Data	
μ (mm^{-1})	0.467
D_x (Mg m^{-3})	1.493
$F(000)$	164
Crystal Size (mm)	0.32 × 0.21 × 0.12
Crystal Habit	Colorless block crystal
Data Collection	
Diffractometer	Bruker APEXII D8 venture, φ and ω-scans
Monochromater	Graphite
Radiation Type, λ(Å)	Mo Kα, 0.71073
T (K)	298
Indexes Range	$-9 \leq h \leq 9$; $-8 \leq k \leq 8$; $-9 \leq l \leq 9$
Measured Reflections	16573
Independent Reflections	880
Observed Refl. with I> 2σ(I)	821
R_{int}	0.086
Refinement	
Refinement on	F^2
Data/Restraints/Parameters	880/0/61
$R[F^2 > 2\sigma(F^2)]$	0.054
$wR(F^2)$	0.160
GooF = S	0.93
$\Delta\rho_{max}/\Delta\rho_{min}$ (e $Å^{-3}$)	0.79/−0.85

2.4. Hirshsfeld Surface Analysis

In order to envisage the intermolecular interactions in the crystal of the title compound, a Hirshfeld surface (HS) analysis [15,16] was carried out by using Crystal Explorer 3.1 [17]. The crystallographic information file (cif) is given as input to the Crystal Explorer program. The d_i (inside) and d_e (outside) characterizes the distances to the Hirshfeld surface from the nuclei, with respect to the relative van der Waals radii. In the HS mapped over d_{norm}, the white surface designates contacts with distances equal to the sum of van der Waals radii, and the red and blue colors represent distances shorter or longer than the van der Waals radii [18].

3. Results and Discussion

3.1. Structure Description

The asymmetric part of the $(C_6H_7N_2O)^+ \cdot Cl^-$ salt consists of a $(C_6H_7N_2O)^+$ cation and Cl^- chloride anion (Figure 1). These ions are organized in the crystal to produce centrosymmetric assemblages with space group $P2_1/m$. This means that organic cations $(C_6H_7N_2O)^+$ and chloride anions are situated in the mirror plane (x, 1/4, z) creating strictly planar layers (Figures 2 and 3). These layers are approximately parallel to each other by π–Cl^- interactions between centroid of pyridinium group and chloride anions (3.46 Å).

The crystal packing is stabilized mainly by three intermolecular N-H···O and N-H···Cl hydrogen bonds. The terminal nitrogen N1 of amide groups is related by one hydrogen bond to the chloride anions (N1-H1A···Cl1). The N2 atom forms two intermolecular hydrogen bonds to chloride anions (N2-H2···Cl1) and to oxygen atoms (N2-H2···O1). Additionally, the cations show two C-H···Cl interactions between the carbon atoms of pyridine rings and the chloride anions (C5-H5···Cl1 and C6-H6···Cl1) (Figure 3). There is also an intramolecular hydrogen bond between O1 and H5 (C5-H5···O1) which promotes also the coplanar arrangement of the amide group with the plane of the aromatic ring. The main characteristics for hydrogen bonds data are listed in Table 2.

Table 2. Hydrogen bonds parameters for $(C_6H_7N_2O)^+ \cdot Cl^-$.

D-H·A	H·A (Å)	D·A (Å)	D-H·A (°)	Symmetry Operations
N1-H1A···Cl1	2.07	2.913 (8)	167	-
N2-H2···Cl1	2.63	3.282 (8)	134	x, y, z−1
N2-H2···O1	2.14	2.799 (2)	133	x, y, z−1
C5-H5···Cl1	2.71	3.537 (8)	148	x+1, y, z−1
C6-H6···Cl1	2.83	3.389 (8)	120	x, y, z−1
C5-H5·O1	2.51	2.982 (4)	112	x,y z−1

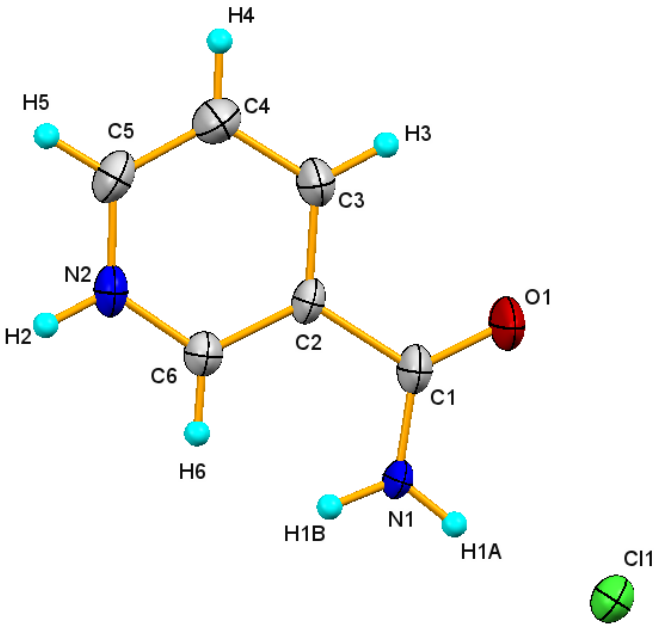

Figure 1. Molecular structure and labeling scheme (50% probability ellipsoids) of the studied salt.

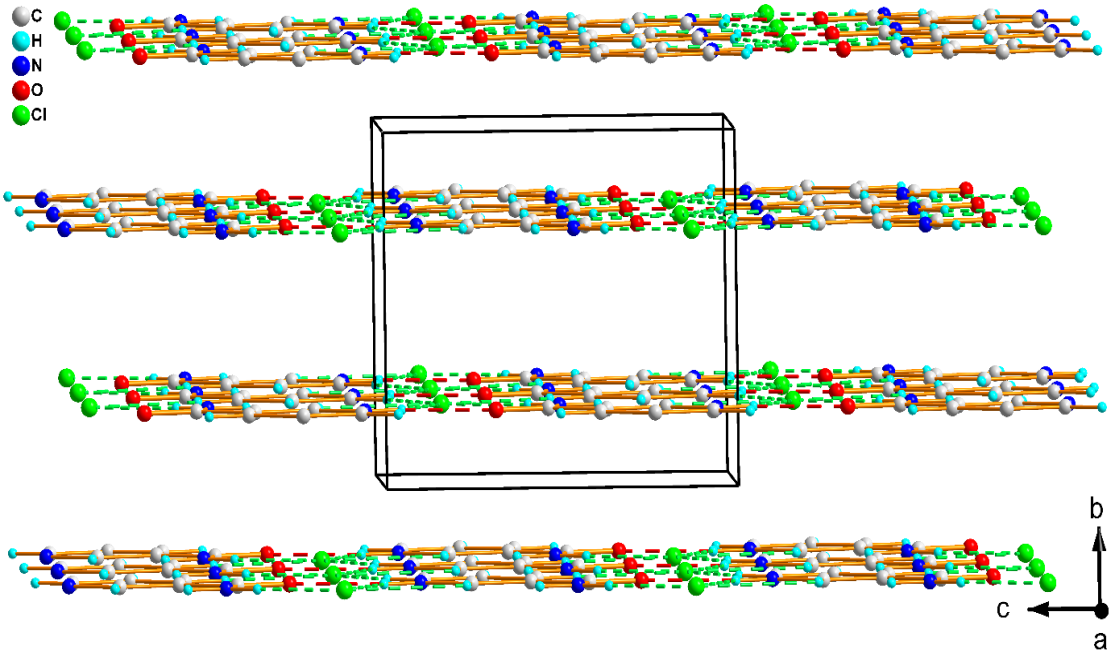

Figure 2. Autostereogram of $(C_6H_7N_2O)^+ \cdot Cl^-$ showing a 2D-layers stacked along the *b*-axis.

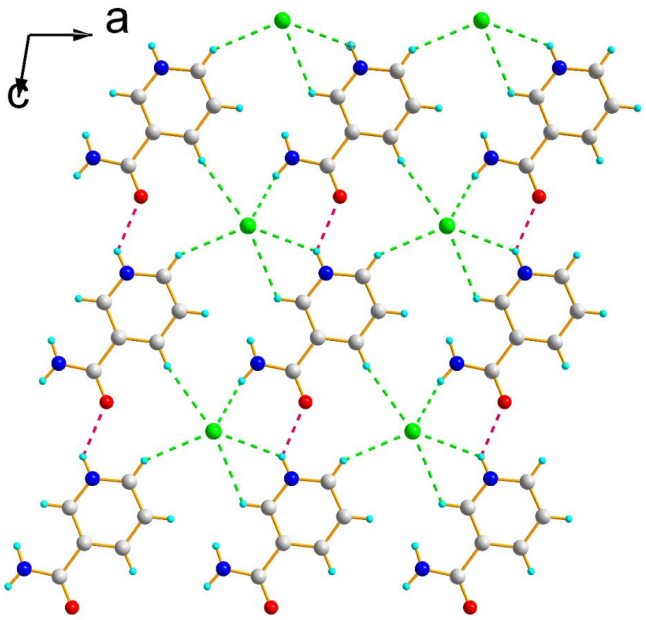

Figure 3. A view along [010] showing organic cations linked by chloride anions via N–H···O (Red), N–H···Cl and C–H···Cl (Green) hydrogen bonds shown as dashed lines.

In the previous polymorph of hydrochloride salt of nicotinamide [19] the cation is also planar but the angle between the planes of the pyridinium and amide moieties is 29.75°. Some nicotinamide-form compounds [20–22] contain amide-amide, amide-chloride and pyridinium-chloride interactions but the title compound shows the equivalent amide-chloride, amide-pyridinium and pyridinium-chloride interactions. In addition, the chloride anions in the title compound contribute to π-Cl^- interaction between two parallel layers but in the other polymorphs act only as hydrogen-bond acceptor atoms between donor atoms of molecules in the same chain, with no further interactions between the chains.

3.2. Crystal Morphology and Packing

The morphology of $(C_6H_7N_2O)^+ \cdot Cl^-$ molecule was predicted using the Materials Studio program [23]. BFDH method is based on geometrical calculations of unit cell dimensions and symmetry operators to define a list of potential growth faces and their eagerness to grow. The aims of BFDH [24–26] law led to the assumption that the size of any face {hkl} is inversely proportional to the inter-planar distance (d_{hkl}) that characterize the family of planes parallel to that face. As a consequence, the thinner the spacing between each repeated face, the faster the growth of a specific face. Thus, faces are classified on the basis of their morphological importance (MI) and generally according to BFDH law, the larger inter-planar distance d_{hkl} is the larger morphological importance of the corresponding hkl face. The combination of all these theories and experimental evidences gives an explanation of the leading role of low Miller indices faces as the morphologically important (MI) faces in the crystal morphology.

The BFDH morphology and crystal morphology observed by SEM was shown in Figure 4. It illustrates that the predicted morphology is very similar to the experimental one. The observed morphology of $(C_6H_7N_2O)^+ \cdot Cl^-$ is that of a bulk crystal (Figure 4b). The calculated results show that the crystal morphology dominated by six faces, (001), (100), (101), (011), (110) and (111). The most important growth surfaces are (001) and (100) which contribute significantly to the surface area. Table 3 summarizes the growth rate and morphological importance of different planes of $(C_6H_7N_2O)^+ \cdot Cl^-$ crystal.

The $(C_6H_7N_2O)^+ \cdot Cl^-$ crystal surfaces have different molecular orientations, as shown in Figure 5. The $(C_6H_7N_2O)^+$ cations on the (001), (100) and (101) faces are organized perpendicular to the crystal plane, while the ones on the (110), (011) and (111) faces are at an angle to the crystal plane.

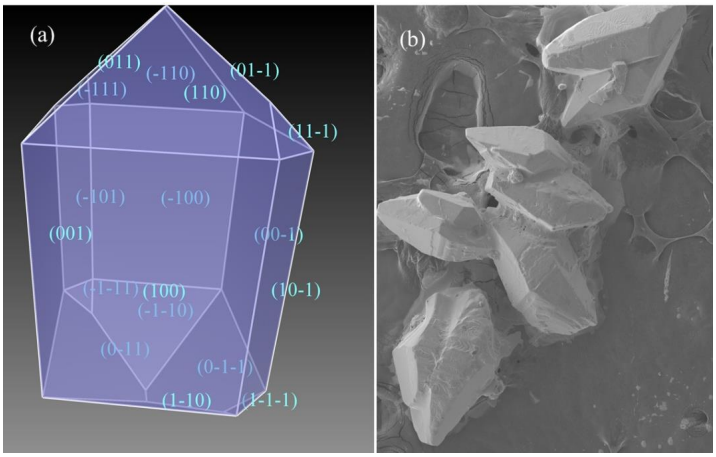

Figure 4. (**a**) BFDH predicted morphology (morphological importance (MI) faces are shown together with their Miller indices) (**b**) Experimental crystal morphology (SEM image).

Table 3. Morphology predictions for the monoclinic structure of $(C_6H_7N_2O)^+ \cdot Cl^-$ by means of Bravais–Friedel–Donnay–Harker (BFDH).

hkl	Multiplicity	D_{hkl} (Å)	% of Total Facet Area
001	2	7.39	27.67
100	2	7.07	26.02
101	2	5.59	6.89
011	4	4.95	20.58
110	4	4.85	17.57
111	4	4.28	1.27

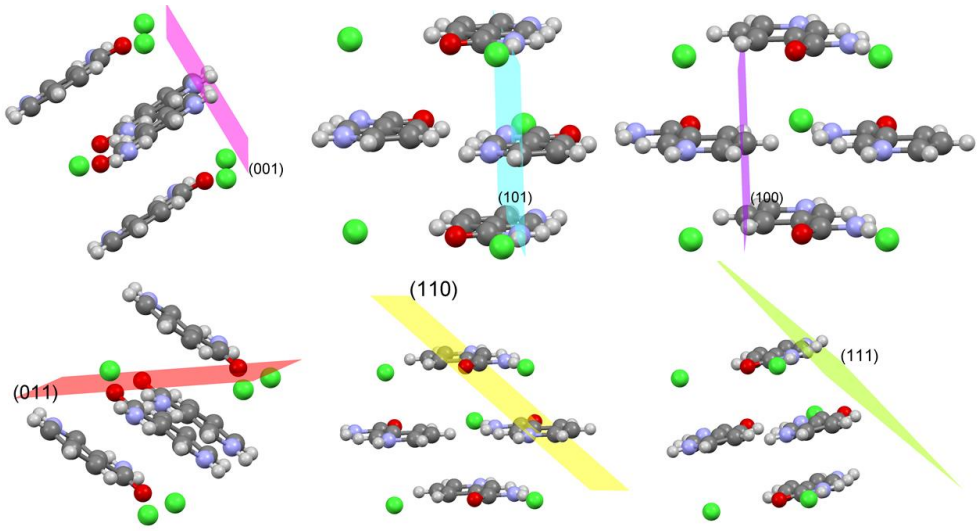

Figure 5. Molecular arrangement of morphologically crystal faces $(C_6H_7N_2O)^+ \cdot Cl^-$. The relative Miller indices are shown together with the respective outcropping atoms.

3.3. Hirshfeld Surface Analysis

The Hirshfeld surfaces of this new polymorph of 1H-nicotineamidium chloride salt and the previous polymorph [19] plotted over d_{norm} in the range −0.487 to 1.029 a. u and −0.537 to 1.105 a. u. are elucidated in Figure S1a and Figure S2a respectively. Information concerning the intermolecular interactions of the studied polymorph, visible as spots on the Hirshfeld surface (Figure S1a), is recapitulated in Table 2. For instance, the distinct circular red spots are due to the N–H···O(Cl) and C–H···Cl contacts, whereas the white spots are due to H···H contacts. The shape-index of the HS is a

tool to visualize the π–π stacking by the presence of adjacent red and blue triangles; if there are no neighboring red and/or blue triangles, then there are no π–π interactions. Figures S1b and S2b clearly show that no π–π interactions are present in the title structure and the previous polymorph. The absence of the π–π interactions in the two polymorphs is also confirmed by the absence of the flat regions on the Hirshfeld surface plotted over curvedness in Figures S1c and S2c. (See Supplementary Materials).

The intermolecular interactions present in the studied polymorph are also observable on the two-dimensional fingerprint plot, which can be decomposed to quantify the individual contributions of each intermolecular interaction involved in the structure. The overall two-dimensional fingerprint plot, Figure 6a, and those defined into H···H, H···Cl/Cl···H, H···O/O···H, H···C/C···H and Cl···C/C···Cl contacts [27] are elucidated in Figure 6b–e, respectively, together with their relative contributions to the Hirshfeld surface. The most important contribution to the overall crystal packing (26.7%) is from H···H interactions, which are shown in Figure 6b as widely scattered points of high density due to the large hydrogen content of the molecule. The fingerprint plot, Figure 6c, defined into H···Cl/Cl···H contacts associated with N(C)–H···Cl hydrogen bonding, which make a 23.5% contribution to the HS, shows a pair of characteristic wings and a pair of spikes with the tips at $d_e + d_i \sim 2.5$ Å. The H···O/O···H contacts in the structure with a 19% contribution to the HS have a symmetrical distribution of points, Figure 6d, with the tips at $d_e + d_i = 2.05$ Å result from the short interatomic N–H···O hydrogen bonding (Table 3). The 17.4% contribution from the C···H/H···C contacts to the Hirshfeld surface, generally slightly preferred in a sample of CH aromatic molecules, results in a symmetric pair of wings, Figure 6e. The Cl···C/C···Cl contacts, which are the measure of π–Cl^- stacking interactions, occupy 6.3% of the Hirshfeld surface and seem to be a unique triangle at about $d_e = d_i \sim 1.7$ Å (Figure 6f). The Hirshfeld surface analysis demonstrates also the existence of other weak intermolecular contacts, for which the percentage participations to the Hirshfeld surface area are low: N···Cl/Cl···N (4.2%), N···C/C···N (1.5%), N···N (0.7%), H···N/N···H (0.6%) and O···C/C···O (0.1%). All these intermolecular contacts mostly contribute to the packing of the new polymorph of 1H-nicotineamidium chloride salt.

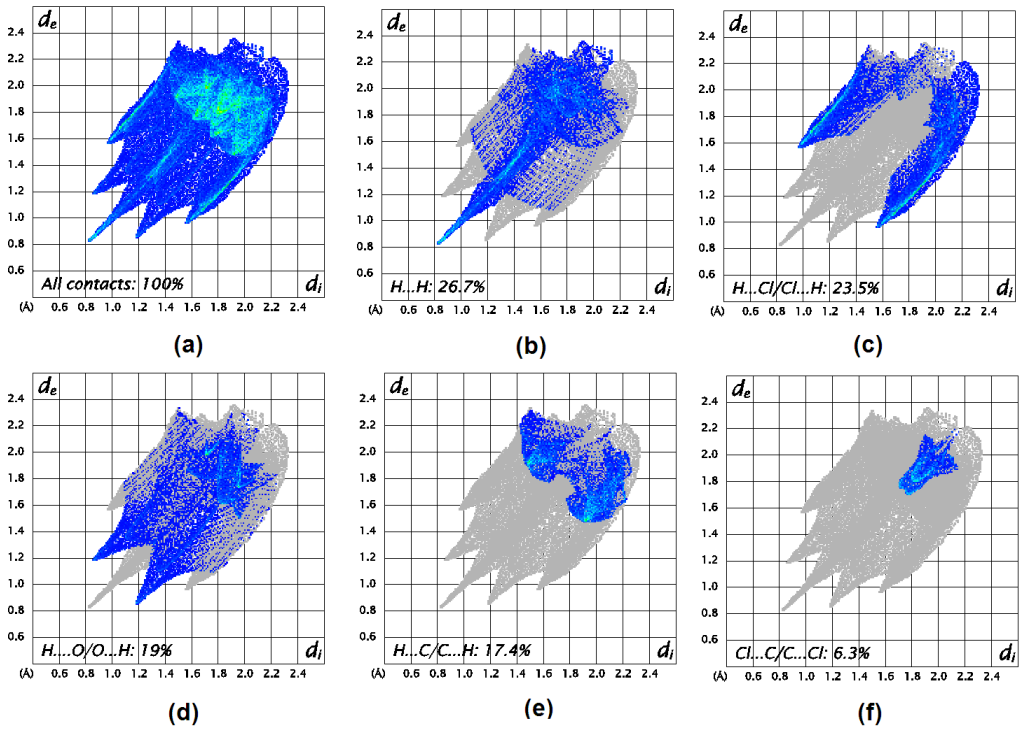

Figure 6. The full two-dimensional fingerprint plots for the title compound, showing (**a**) all interactions, and delineated into (**b**) H···H, (**c**) H···Cl/Cl···H, (**d**) H···O/O···H, (**e**) H···C/C···H and (**f**) Cl···C/C···Cl. The d_i and d_e values are the closest internal and external distances (in Å) from given points on the Hirshfeld surface.

Compared with the newly polymorph, the two-dimensional fingerprint plot of the previous polymorph (Figure S3e,f) shows that the main contribution to the overall crystal packing comes from H···Cl/Cl···H (30.6%). In addition, the C···C/Cl···C contacts represent only 0.4%. These results are in good agreement with the structural study of the old polymorph in which the structure was dominated by the N-H···Cl hydrogen bonds with absence of π–Cl^- stacking interactions. Figure 7 shows the percentage contributions of the various contacts in the two polymorphs.

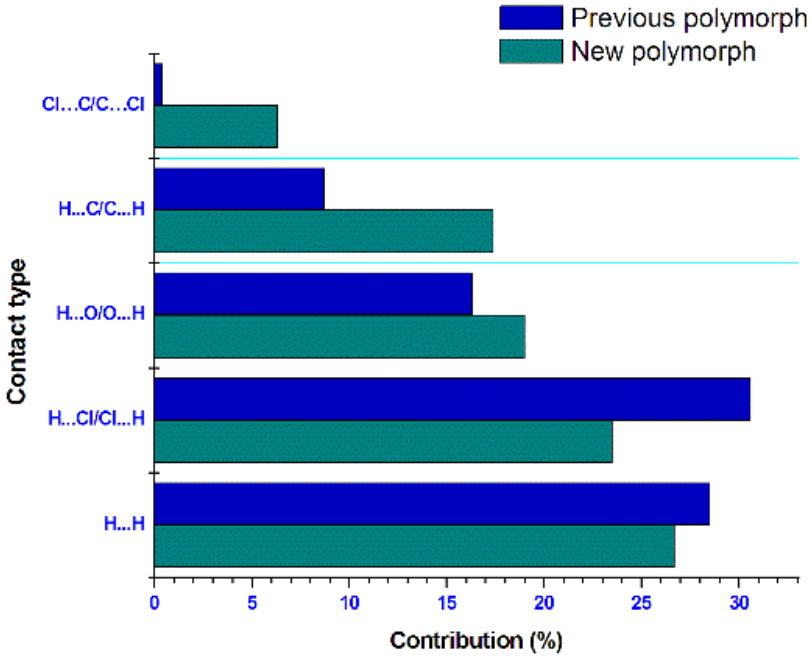

Figure 7. Relative contribution (%) of various intermolecular interactions to the Hirshfeld surface area of the two polymorphs.

4. Conclusions

A new organic salt $(C_6H_7N_2O)^+ \cdot Cl^-$ has been synthesized by slow evaporation method at room temperature. The single crystal X-ray diffraction was carried out in order to perform structural analysis. The crystal structure of the title salt is stabilized by N-H···O, N–H···Cl and C-H···Cl hydrogen bonds. Moreover, the protonated organic cations and the chloride anions show a π-Cl^- interaction enhancing stability to the two-dimensional architecture. The crystal morphology of $(C_6H_7N_2O)^+ \cdot Cl^-$ has successfully been predicted using BFDH and shows a big similarity with the experimental one. The main crystal faces (001), (100), (101), (011), (110) and (111) are dominant in predicted morphology bulk. Hirshfeld surface analysis revealed that H···H (26.7%), H···Cl/Cl···H (23.5%), H···O/O···H (19%) and H···C/C···H (17.4%) contacts appear to be a major contributor in the crystal packing.

Supplementary Materials: The following are available online at http://www.mdpi.com/2073-4352/9/11/571/s1, Figure S1: View of the three-dimensional Hirshfeld surface of the new polymorph plotted over (a) d_{norm}, (b) shape-index and (c) curvedness, Figure S2: View of the three-dimensional Hirshfeld surface of the previous polymorph [19] plotted over (a) d_{norm}, (b) shape-index and (c) curvedness, Figure S3: The full two-dimensional fingerprint plots of the previous polymorph [19], showing (a) all interactions, and delineated into (b) H···H, (c) H···Cl/Cl···H, (d) H···O/O···H, (e) H···C/C···H and (f) Cl···C/C···Cl. The d_i and d_e values are the closest internal and external distances (in Å) from given points on the Hirshfeld surface.

Author Contributions: Crystal growth and manuscript writing, H.F.; software and validation H.C.; analysis, O.S.A. and S.A.A.-H.; English checking A.G.

Funding: This research received no external funding.

Conflicts of Interest: The authors declare no conflict of interest.

References

1. Ganguly, P.; Desiraju, G.R. Van der Waals and Polar Intermolecular Contact Distances: Quantifying Supramolecular Synthons. *Chem. Asian J.* **2008**, *3*, 868–880. [CrossRef]
2. Nangia, A. Conformational Polymorphism in Organic Crystals. *Acc. Chem. Res.* **2008**, *41*, 595–604. [CrossRef]
3. Hulme, A.T.; Johnston, A.; Florence, A.J.; Fernandes, P.; Shankland, K.; Bedford, C.T.; Welch, G.W.; Sadiq, G.; Haynes, D.A.; Motherwell, W.D.S.; et al. Search for a Predicted Hydrogen Bonding Motif—A Multidisciplinary Investigation into the Polymorphism of 3-Azabicyclo[3.3.1]nonane-2,4-dione. *J. Am. Chem. Soc.* **2007**, *129*, 3649–3657. [CrossRef]
4. Price, S.L. From Crystal Structure Prediction to Polymorph Prediction: Interpreting the Crystal Energy Landscape. *Phys. Chem. Chem. Phys.* **2008**, *10*, 1996–2009. [CrossRef]
5. Vallejos, M.M.; Angelina, E.L.; Peruchena, N.M. Bifunctional Hydrogen Bonds in Monohydrated Cycloether Complexes. *J. Phys. Chem. A.* **2010**, *114*, 2855–2863. [CrossRef]
6. Jin, S.; Wang, D.J. Hydrogen Bonded 3D Supramolecular Architectures of Three Saccharinate Salts. *Chem. Crystallogr.* **2011**, *41*, 1085–1092. [CrossRef]
7. Korotkovaa, E.I.; Kratochvíl, B. Pharmaceutical Cocrystals. *Procedia Chem.* **2014**, *10*, 473–476. [CrossRef]
8. Lu, J.; Rohani, S. Preparation and Characterization of Theophylline−Nicotinamide Cocrystal. *Org. Process Res. Dev.* **2009**, *13*, 1269–1275. [CrossRef]
9. Lemmerer, A.; Esterhuysen, C.; Bernstein, J. Synthesis, Characterization, and Molecular Modeling of A Pharmaceutical Co-Crystal: (2-Chloro-4-Nitrobenzoic Acid):(Nicotinamide). *J. Pharm. Sci.* **2010**, *99*, 4054–4071. [CrossRef]
10. Bathori, N.B.; Lemmerer, A.; Venter, G.A.; Bourne, S.A.; Caira, M.R. Pharmaceutical Co-crystals with Isonicotinamide-Vitamin B3, Clofibric Acid, and Diclofenac-and Two Isonicotinamide Hydrates. *Cryst. Growth Des.* **2011**, *11*, 75–87. [CrossRef]
11. Fábián, L.; Hamill, N.; Eccles, K.S.; Moynihan, H.A.; Maguire, A.R.; McCausland, L.; Lawrence, S.E. Cocrystals of Fenamic Acids with Nicotinamide. *Cryst. Growth Des.* **2011**, *11*, 3522–3528. [CrossRef]
12. Sheldrick, G.M. SHELXT—Integrated space-group and crystal-structure determination. *Acta Crystallogr. A* **2015**, *A71*, 3–8. [CrossRef]
13. Sheldrick, G.M. Crystal structure refinement with SHELXL. *Acta Crystallogr. C* **2015**, *C71*, 3–8. [CrossRef]
14. Brandenburg, K. *DIAMOND*; Crystal Impact GbR: Bonn, Germany, 2006.
15. Hirshfeld, H.L. Bonded-atom fragments for describing molecular charge densities. *Theor. Chim. Acta* **1977**, *44*, 129–138. [CrossRef]
16. Spackman, M.A.; Jayatilaka, D. Hirshfeld surface analysis. *Cryst. Eng. Comm.* **2009**, *11*, 19–32. [CrossRef]
17. Wolff, S.K.; Grimwood, D.J.; McKinnon, J.J.; Turner, M.J.; Jayatilaka, D.; Spackman, M.A. *Crystal Explorer version 3.1*; University of Western Australia: Perth, Australia, 2012.
18. Venkatesan, P.; Thamotharan, S.; Ilangovan, A.; Liang, H.; Sundius, T. Crystal structure, Hirshfeld surfaces and DFT computation of NLO active (2E)-2-(ethoxycarbonyl)-3-[(1-methoxy-1-oxo-3-phenylpropan-2-yl)amino] prop-2-enoic acid. *Spectrochim. Acta Part A* **2016**, *153*, 625–636. [CrossRef]
19. Gubin, A.I.; Nurakhmetov, N.N.; Buranbaev, M.Z.; Mulkina, R.I.; Erkasov, R.S. Crystal and molecular structure of nicotinamide hydrochloride. Donor-acceptor properties of protonated nicotinamide. *Kristallografiya (Russ.) (Crystallogr. Rep.)* **1989**, *34*, 238–239.
20. Delgado, G.E.K.; Varela, N.; Mora, A.J.; Colmenárez, J.B.; Atencio, R. Synthesis, Thermal Studies, Spectroscopy Characterization, and Crystal Structure of Nicotinamidium Oxamate. *Mol. Cryst. Liq. Cryst.* **2015**, *609*, 218–227. [CrossRef]
21. Oswald, I.D.H.; Motherwell, W.D.S.; Parsons, S. A 1:2 co-crystal of isonicotinamide and propionic acid. *Acta Crystallogr. E* **2004**, *60*, 2380–2383. [CrossRef]
22. Perumalla, S.R.; Sun, C.C. Design and Synthesis of Solid State Structures with Conjugate Acid-Base Pair Interactions. *Cryst. Eng. Comm.* **2012**, *14*, 3851–3853. [CrossRef]
23. *Materials Studio, Version 7.0*; Accelrys Software Inc.: San Diego, CA, USA, 2013.
24. Bravais, A. *Etudes Crystallographiques*; Academi des Sciences: Paris, France, 2010.
25. Donnay, J.D.H.; Harker, D. A new law of crystal morphology extending the Law of Bravais. *Am. Mineral.* **1937**, *22*, 446–467.

26. Prywer, J. Morphological importance of crystal faces in connection with growth rates and crystallographic structure of crystal. *Cryst. Growth Des.* **2002**, *2*, 281–286. [CrossRef]
27. McKinnon, J.J.; Jayatilaka, D.; Spackman, M.A. Towards quantitative analysis of intermolecular interactions with Hirshfeld surfaces. *Chem. Commun.* **2007**, *37*, 3814–3816. [CrossRef] [PubMed]